



Published in final edited form as:

*IEEE Trans Neural Syst Rehabil Eng.* 2016 April ; 24(4): 413–423. doi:10.1109/TNSRE.2015.2415811.

## The Retinal Response to Sinusoidal Electrical Stimulation

Perry Twyford and Shelley Fried [Member, IEEE]

VA Boston Healthcare System and the Department of Neurosurgery, Massachusetts General Hospital and Harvard Medical School, Their Research Building, Rm 415, 55 Fruit St. Boston, MA, 02114 USA.

### Abstract

Rectangular electrical pulses are the primary stimulus waveform used in retinal prosthetics as well as many other neural stimulation applications. Unfortunately, the utility of pulsatile stimuli is limited by the inability to avoid the activation of passing axons which can result in the distortion of the spatial patterns of elicited neural activity. Because avoiding axons would likely improve clinical outcomes, the examination of alternate stimulus waveforms is warranted. Here, we studied the response of rabbit retinal ganglion cells (RGCs) to sinusoidal electrical stimulation applied at frequencies of 5, 10, 25, and 100 Hz. Targeted RGCs were restricted to 4 common types: OFF-Brisk Transient, OFF-Sustained, ON-Brisk Transient, and ON-Sustained. Interestingly, response patterns varied between different types; the most notable difference was the relatively weak response of ON-Sustained cells to low frequencies. Calculation of total spike counts per trial revealed that lower frequencies are more charge efficient than high frequencies. Finally, experiments utilizing synaptic blockers revealed that 5 and 10 Hz activate photoreceptors while 25 and 100 Hz activate RGCs. Taken together, our results suggest that while sinusoidal electrical stimulation may provide a useful research tool, its clinical utility may be limited.

### Keywords

Electrical Stimulation; Retina; Retinal Prosthesis; Sinusoidal

## I. Introduction

Outer retinal diseases such as macular degeneration and retinitis pigmentosa are characterized by degeneration of the light-sensitive photoreceptors in the retina, resulting in vision loss and eventual blindness. Microelectronic retinal prosthetics attempt to restore vision by bypassing the damaged retinal layers and stimulating activity directly in the inner retinal neurons. Multiple devices are currently undergoing clinical trials in human patients [1, 2], while still more are in various stages of development [3-7]. Although several devices can reliably elicit visual percepts, elicited vision is often poor in quality and inconsistent across patients [8, 9]. Several factors are thought to limit the quality of artificial vision, but it is likely that suboptimal stimulation methods contribute to the imperfect clinical outcomes.

Pulsatile waveforms have been the primary stimuli used in retinal implants thus far [1, 9], likely due to the early successes of such waveforms in other neural stimulation applications including cochlear implants [10], deep brain stimulation [11], and pacemakers [12]. However, pulses can be problematic because they not only activate targeted neurons, but also activate axons of passage, and therefore can expand the spatial extent of activation beyond the immediate vicinity of the stimulating electrode [13, 14]. Short duration pulses tend to only activate ganglion cells and axons, while longer duration pulses also activate presynaptic neurons, e.g. bipolar cells and/or photoreceptors [15-17]. Activation of such neurons can lead to spiking in the ganglion cell and is referred to as indirect or network-mediated activation. The short processes of bipolar cells and photoreceptors confines the network-mediated component of the response to a relatively small focal region around the stimulating electrode, and therefore is likely to better replicate the spatial elements of a given visual scene than direct activation. Note that photoreceptors do not survive the degeneration process and as such are not considered a viable target for clinical applications (but see [18]). Thus, a stimulus that activates bipolar cells without simultaneously activating ganglion cells or their axons would be ideal for creating focal activity.

Direct activation of ganglion cells arises when voltage-gated sodium channels within the cell membrane become activated by the stimulus; the proximal portion of the axon contains the highest density of channels and is the region most sensitive to stimulation [14, 19, 20]. Voltage-gated sodium channels are maximally activated by abrupt changes in membrane voltage, suggesting that stimulus waveforms which cause membrane voltage to change gradually will not effectively activate ganglion cells. In contrast to ganglion cells, bipolar cells and photoreceptors do not contain similar densities of sodium channels and as such are less sensitive to transient depolarizations. Instead, these neurons respond to longer duration stimuli, probably because their activation is mediated by ion channels that have longer time constants [21]. Consistent with these findings, low frequency sinusoidal waveforms were shown to activate the network (bipolar cells and/or photoreceptors) with thresholds that were at least an order of magnitude lower than the thresholds for activating passing axons [22]. This is potentially highly advantageous and is in contrast to stimulation with long-duration pulses, in which thresholds mediated through the network were *comparable* to those for axonal activation when the stimulating electrode was positioned epiretinally [23]. While this suggests that low frequency sinusoids may be ideal for avoiding axons and confining activation, recent studies suggest that photoreceptor activation may contribute to the responses arising from long-duration sinusoids [22]. If so, this type of approach would be of only limited use in the degenerate retina (e.g. with no photoreceptors available to target), making it important to determine with certainty the neuronal targets of different frequencies of sinusoidal stimulation. While the previous study with sinusoids was able to determine that low frequency sinusoids were activating presynaptic neurons, the study did not unequivocally identify whether bipolar cells or photoreceptors were activated at each frequency.

In addition to identifying the targets of stimulation at each stimulus frequency, several additional concerns must be addressed before low frequency sinusoidal waveforms can be considered suitable for use in a clinical device. For example, the long periods associated with low frequency sinusoidal waveforms can deliver high levels of charge, leading to high

charge-density levels and relatively fast depletion of the battery. It is therefore important to compare the effectiveness across the spectrum of low frequencies under evaluation so as to maximize efficiency. Another concern is that RGC responses to pulsatile stimulation have been shown to desensitize over the course of repeated stimuli [24-26] and therefore it will be necessary to determine if the same holds true for sinusoidal stimulation. Finally, different types of RGCs (transient, sustained, directionally selective, etc.) each code for a different aspect of the visual scene and exhibit highly dissimilar spiking patterns in response to light; it is therefore important to determine how each type of RGC responds to sinusoidal stimuli as such knowledge may enable the creation of spiking patterns that more closely match the natural retinal code.

Here we investigated the use of sinusoidal electrical stimulation for use in a retinal prosthetic. We first classified targeted RGCs into known physiological types so that responses to sinusoidal stimuli could be compared across types. We also examined the charge efficiency at each stimulation frequency. Finally, we applied multiple types of synaptic blockers in order to fully resolve the cellular targets of sinusoidal stimulation at each frequency.

## II. Methods

### A. Animal preparation and retina isolation

The care and use of animals followed all federal and institutional guidelines and all protocols were approved by the Institutional Animal Care and Use Committees of the VA Boston Healthcare System and/or the Subcommittee of Research Animal Care of Massachusetts General Hospital. Female New Zealand white rabbits (~2.5 kg) were anesthetized with injections of xylazine/ketamine and subsequently euthanized with an intracardial injection of sodium pentobarbital. Immediately after death, the eyes were removed. All procedures following eye removal were performed under dim red illumination. The front of the eye was removed, the vitreous was eliminated, and the eye cup dissected so that the retina could be flattened. The retina was separated from the retinal pigment epithelium and mounted, photoreceptor side down, to a 10-mm square piece of Millipore filter paper (0.45  $\mu\text{m}$  HA Membrane Filter) that was mounted with vacuum grease to the recording chamber (~1.0 ml volume). A 2 mm circle in the center of the Millipore paper allowed light from below to be projected onto the photoreceptors.

### B. Electrophysiology and Light responses

Glass patch pipettes were used to make small holes in the inner limiting membrane and ganglion cells were targeted under visual control. Spiking was recorded with a cell-attached patch electrode (8–12  $M\Omega$ ), filled with Ames medium (Sigma Aldrich, A1420). Two silver-chloride coated silver wires served as the ground and were positioned at opposite edges of the recording chamber, each ~15 mm from the targeted cell.

The stimulus and data acquisition software was controlled by custom software written in LabView (National Instruments) and Matlab (Mathworks) and written by G. Spor, T. Muench, D. Balya, D. Freeman and M. Im. The sampling rate of the data acquisition setup

was 100 kHz, and the time resolution of the stimulus generator was 50 kHz. Light stimuli were projected onto the retina from below through a liquid crystal display projector (Dell), and focused onto the outer segments of the photoreceptors. A photopic background intensity was maintained throughout the experiment ( $\sim 4$  nW/mm<sup>2</sup>) [27]. Light stimuli consisted of stationary flashed squares (size range: 100–1,000  $\mu$ m), 1 s duration, centered at the soma. Cells were classified as brisk transient (BT) if they responded with high frequency and transient ( $< 500$  ms) bursts of spiking to stimuli centered in their receptive field [27–29]. Consistent with previous reports, BT-cells responded strongest to larger light squares ( $> 500$   $\mu$ m) and responded less or not at all to small squares ( $< 100$   $\mu$ m). Cells were classified as brisk sustained (SUST) if they maintained elevated spiking levels for longer than 500 ms after the luminance change; this classification was used for both ON and OFF RGCs. All cells used in this study were either OFF-BT ( $n = 15$ ), OFF-SUST ( $n = 7$ ), ON-BT ( $n = 11$ ), or ON-SUST ( $n = 7$ ): all other cell types were avoided.

Pharmacological agents were applied to the bath via the switching of a three-way valve, ensuring a continuous flow of perfusion. Synaptic blockers were either AP-4 (40  $\mu$ M L-(+)-2-Amino-4-phosphonobutyric acid) or CdCl<sub>2</sub> (250  $\mu$ M Cadmium Chloride hemipentahydrate), and were perfused into the bath for 5 minutes before responses were taken. Elimination of the light response was used to confirm drug effectiveness. While multiple cells were recorded from each retinal preparation, synaptic blockers were only used for the final cell of each preparation. In cells where both AP-4 and CdCl<sub>2</sub> were used, AP-4 was always applied first.

### C. Electric Stimulation

Electric stimulation was delivered via a 10 k $\Omega$  Platinum-Iridium electrode (MicroProbes); the exposed area was conical with an approximate height of 125  $\mu$ m and base diameter of 15  $\mu$ m, giving a surface area of  $\sim 5,900$   $\mu$ m<sup>2</sup>, comparable to the area of a 40  $\mu$ m disk electrode. The height of the stimulating electrode remained fixed 25  $\mu$ m above the inner limiting membrane; the distance was calibrated by touching the surface of the inner limiting membrane with the tip of the electrode and then using the micromanipulator to raise the height by 25  $\mu$ m. Two silver-chloride coated silver wires served as the return; each was positioned  $\sim 8$  mm from the targeted cell and  $\sim 12$  mm from one another. The stimulating electrode was centered over the axon initial segment on the proximal axon at the approximate site of lowest threshold. It was generally located between 20 and 60  $\mu$ m from the soma along the proximal axon [14, 19, 20]. Using an iterative process, we were able to quickly find the center of the low-threshold region; movement of the stimulating electrode toward the center resulted in decreasing thresholds while movement away from the center resulted in increasing thresholds. The stimulus used during this process was a biphasic pulse (100  $\mu$ s per phase with 100  $\mu$ s inter-phase interval) applied at 10 PPS. Once identified, the stimulating electrode remained fixed over this location for the duration of the experiment.

Electrical stimuli were controlled by Multi-Channel Systems STG2004 hardware and software, and were sinusoidal at frequencies of 5, 10, 25, and 100 Hz. Previous work determined the maximum amplitude that could be used at each frequency (4, 9, 18, and 36  $\mu$ A, respectively) without exceeding the charge density limits of the stimulating electrode

[22, 30]; amplitudes remained fixed at these levels for all experiments. Because we recorded in voltage clamp mode, measurements were of membrane current. Therefore the polarities of the stimulus artifacts appear inverted in the recordings: anodal (+) phases appear as negative, while cathodal (–) phases appear as positive. To remove the sinusoidal electrical artifact (Fig. 1A), a notch filter was used at the frequency of stimulation with a width of 0.2 Hz; the signal-to-noise ratio of action potentials was then large enough to facilitate simple spike detection via threshold crossing. All processing was performed in Matlab (MathWorks).

### III. Results

We recorded spiking activity from retinal ganglion cells (RGCs) in response to electrical stimuli from an extracellular epiretinal electrode (Methods). Stimulus waveforms were sinusoidal with frequencies of 5, 10, 25, or 100 Hz, and were applied continuously for 5 seconds at amplitudes of 4, 9, 18, or 36  $\mu\text{A}$ , respectively; these values were determined to be below the charge density limits of the electrode material [22], and are within the safe limits for both the electrode and surrounding tissue.

We measured responses in 4 different types of RGCs, OFF-Brisk Transient (OFF-BT,  $n = 15$ ), OFF-Brisk Sustained (OFF-SUST,  $n = 7$ ), ON-Brisk Transient (ON-BT,  $n = 11$ ), and ON-Brisk Sustained (ON-SUST,  $n = 7$ ). The use of loose cell-attached patch clamp recordings allowed action potentials to be reliably detected within the sinusoidal stimulation artifact (Fig. 1A).

To better visualize the activity patterns across the full 5-second stimulus, we extracted spike times as a function of the sinusoidal phase during which they occurred, and compiled these into a single plot (Fig. 1B) where each vertical dash represents an action potential and the response to each period of the stimulus is displayed on a separate row (bottom row is 1<sup>st</sup> period). The three periods shown in Fig. 1A are indicated with arrows in Fig. 1B. We refer to this plot as a period overlay; the sinusoidal waveform is superimposed on these plots so that elicited activity can be correlated to the phase of the sinusoid during which it occurs. Viewing the responses in this form allows us to examine the relative phases at which activity was created (spike phases), and determine the consistency of these phases across the duration of the 5-second stimulus. The inset shows an expanded view of the initial portion of the first five periods (grey square), and reveals that the spike phases of the first period were often delayed relative to those of subsequent periods. Examining period overlays across multiple cells of the same type revealed high levels of similarity in the activity patterns created by each RGC type. Fig. 2 shows period overlays from five different OFF-BT cells stimulated at 5 Hz (left column) and five different ON-BT cells stimulated at 10 Hz (right column). Other RGC types and stimulus frequencies showed comparable levels of similarity across responses.

Period overlays of typical responses are shown in Fig. 3 for each of the 4 RGC types at the frequencies indicated. A comparison of the different panels in Fig. 3 reveals five interesting properties of the responses to sinusoidal stimulation: (1) Three cell types, OFF-BT, OFF-SUST, and ON-BT (top 3 rows) exhibited regular spiking that occurred at the same phase of each period throughout the duration of the stimulus. (2) The fourth cell type, ON-SUST,

exhibited activation patterns that were weak and inconsistent at low frequencies (5 and 10 Hz), although the activity became more regular at higher frequencies (25 and 100 Hz). (3) The patterns in both OFF types (BT and SUST) were quite similar at all frequencies tested. This may be a significant limitation towards the goal of trying to re-create physiological signaling patterns with sinusoidal stimulation. (4) At low frequencies, there were differences in the sinusoidal phase at which spikes occurred for ON vs. OFF-BT cells; we refer to such differences as phase differences. The observed phase differences are consistent with previous work [22], and are analyzed in more detail below. (5) While most responses occurred at a constant phase throughout the duration of the stimulus, some responses demonstrated an accommodative effect. The defining feature of this effect was that spike phases were progressively delayed until a phase was reached that remained constant across subsequent periods; this appears as a curved shape at the bottom of the plot and can be seen in the OFF-BT response to 100 Hz stimulation (Fig. 3, top right panel). We did not further investigate the cellular mechanisms behind this response property.

Because it is highly desirable to minimize the charge used for each stimulus, thus extending battery life of the device, we explored the charge efficiency of each frequency; this was done by calculating the amount of activity produced per unit of charge for each response. The spike raster plots of Fig. 4A show the activity patterns for a single OFF-BT cell in response to sinusoidal stimuli at the frequencies indicated, where each vertical line represents an action potential. While the 100 Hz raster appears to contain the largest number of spikes, each burst of activity in the 5 Hz raster contained spikes with a much lower inter-spike interval than those at 100 Hz; this made visual comparison of activity levels unreliable. Therefore, the average total number of spikes produced per 5-second stimulus was determined for each cell type; the results are presented in Fig. 4B. ON-SUST cells exhibited substantially less spiking than the other three RGC types at low frequencies (5 and 10 Hz), but spike counts increased at higher frequencies. There was not a statistically significant trend in the activity levels for the other types as frequency increased from 5 to 100 Hz.

The average number of spikes per period was also determined and plotted for each cell in Fig. 4C, where the vertical bars that represent individual cells are arranged in order of ascending spike count within each RGC type (OFF-BT, OFF-SUST, ON-BT, and ON-SUST, from left to right, respectively). The averages of all values in Fig. 4C were calculated for each RGC cell type and were plotted as a function of stimulus frequency in Fig. 4D. As expected, the number of spikes per period decreased with increasing frequency. The plots also confirm that OFF-BT, OFF-SUST, and ON-BT cells showed highly similar amounts of elicited activity, while ON-SUST cells produced far fewer spikes than the other cell types, particularly at low frequencies. Fig. 4E shows the average spikes per period for OFF-BT, OFF-SUST, and ON-BT (solid line, left axis); ON-SUST cells were not included in this analysis. Using the values of average spikes per period, we calculated the charge per spike for each frequency, and plotted this on the same plot (dotted line, right axis). The charge per spike curve suggests less charge per spike is necessary at low frequency stimulation than at high frequency, and therefore implies that low frequency stimulation is more efficient.

One of the most interesting aspects of sinusoidal stimulation is the ability to create activity at different phases of the sinusoidal waveform for different RGC types. In order to examine



this phenomenon further, we determined the average phase at which the first spike occurred for each response, referred to as the mean first spike phase: an example is shown in the inset of Fig. 5A, where the calculated mean first spike phase is indicated by the small arrow. Mean first spike phases were plotted for each cell as a function of stimulus frequency (Fig. 5A) - OFF cells are plotted on the left and ON cells on the right. The data point indicated by the large arrow arises from the period overlay shown in the inset, and serves as a sample calculation. OFF-SUST and OFF-BT cells showed highly similar response phases and could not be distinguished by the appearance of their phase vs. frequency curves. ON-SUST and ON-BT curves were slightly different (as indicated), although it is important to remember that ON-SUST cells produced very little activity at 5 and 10 Hz (see Fig. 4). As such, plotted values were derived from responses in which spikes were often sparse and highly irregular (example shown in Fig. 3).

Fig. 5B shows the average of the mean first spike phases for all ON and OFF-BT cells. The plots reveal large phase differences, particularly at low frequencies. At 5 Hz, the phase difference was  $\sim 160^\circ$ , with ON cells being activated during the anodal phase and OFF cells during the cathodal phase. This change in phase likely arises from the sign-inverting metabotropic glutamate receptors found on the photoreceptor-to-bipolar synapse of the ON pathway [22]. Because of this sign-inverting synapse, hyperpolarization of the ON photoreceptors (presumably occurring in response to the anodal phase of the 5 Hz sinusoid) would lead to depolarization of ON bipolar cells and ultimately lead to spiking in the ON RGC. In contrast, depolarization of the ON photoreceptors (during cathodal stimulation) hyperpolarizes ON bipolar cells and therefore generates little or no spiking in ON RGCs. The large phase difference between ON and OFF-BT cells at 10 Hz ( $\sim 143^\circ$ ) similarly suggests that photoreceptors are the neurons that respond to 10 Hz sinusoids. At 25 Hz, the phase difference between ON and OFF-BT cells was  $\sim 93^\circ$ , with both responses occurring during the cathodal phase. This phase difference can also be observed in the period overlays shown in Fig. 3, where the ON-BT response exhibited spikes on the rising phase of the positive portion of the waveform, while the OFF-BT response exhibited spikes on the falling phase. Because spiking occurred during the cathodal phase for both ON and OFF BT cells, this  $\sim 90^\circ$  phase difference is not likely a result of photoreceptor activation (and thus the sign-inverting synapse), but instead from some other difference between the ON and OFF BT pathways.

Average mean first spike phases were also compared for ON and OFF-SUST cells (Fig. 5C). While some phase differences were seen between SUST-type cells, the differences at low frequencies were not as robust as those between BT-type cells. Again, the inconsistent activity patterns elicited in ON-SUST cells in response to low frequency stimulation likely contributes to this result.

To unequivocally identify the cellular targets of sinusoidal stimulation at each frequency, we utilized the synaptic blockers AP-4 and CdCl<sub>2</sub> (40  $\mu$ M and 250  $\mu$ M, respectively, Methods). AP-4 is an agonist of the metabotropic glutamate receptor (mGluR6) and is known to block transmission through the photoreceptor-to-bipolar synapse in the ON pathway [31-33], while CdCl<sub>2</sub> blocks all synaptic transmission to the RGC [34]. Fig. 6A shows period overlays of the responses of an ON-BT cell under control conditions (top row), with photoreceptor input

to ON bipolar cells blocked via AP-4 (middle row), and with all synaptic input blocked with CdCl<sub>2</sub> (bottom row).

At 5 Hz, the strong response in ON cells that occurred during the anodal phase under control conditions was eliminated in the presence of AP-4. However, weaker spiking was then elicited occurring during the cathodal phase. The change in phase that occurred when photoreceptor input is blocked supports the notion that the response to 5 Hz stimulation in ganglion cells (under control conditions) results from photoreceptor activation. The activity during the cathodal phase that occurred in the presence of AP-4 was eradicated with the addition of CdCl<sub>2</sub>, indicating that such activity arose through synaptic input and therefore is most likely the result of bipolar cell activation. Thus our results suggest that 5 Hz stimulation can activate both photoreceptors and bipolar cells, but that photoreceptor mediated activation is the dominant response under control conditions (Discussion). At 10 Hz, response patterns in ON cells were generally similar to those arising in response to 5 Hz. The most significant difference was the persistence of spiking in the presence of CdCl<sub>2</sub>, suggesting ganglion cells can be activated directly by 10 Hz stimulation. The response in the presence of CdCl<sub>2</sub> was less robust than the response in AP-4, suggesting the AP-4 response arises from both bipolar cell and RGC activation. Taken together, these results indicate that 10 Hz is capable of activating photoreceptors, bipolar cells and RGCs, although the response under control conditions is dominated by the photoreceptor-mediated component. Responses to 25 Hz stimulation showed only small changes in the presence of either blocker, suggesting that they arose primarily through direct activation of the RGC. There were small decreases in the level of spiking that occurred with the addition of each blocker. For example, in Fig. 6A, ~7 spikes per period were elicited under control conditions, ~6 in AP-4, and ~5 in CdCl<sub>2</sub>. These slight decreases were observed for all cells tested (n = 4, p=6.58E<sup>-5</sup> control to AP-4, p = 2.53E<sup>-5</sup> AP-4 to CdCl<sub>2</sub>, *paired t-test*). These small decreases in activity suggest that 25 Hz, while producing strong direct activation in the RGC, also produces a response in multiple classes of presynaptic retinal neurons (Discussion). Finally, responses to 100 Hz remained largely unchanged in the presence of all pharmacological blockers, suggesting that the observed activity arose through direct activation of the RGC only.

Responses of an OFF-BT cell to sinusoidal stimulation are shown in Fig. 6B under control conditions (top row) and in the presence of CdCl<sub>2</sub> (bottom row). AP-4 was not used for OFF cells as it does not block the photoreceptor-bipolar cell synapse in the OFF pathway. Further, the lack of ON pathway inhibition via AP-4 can cause tonic depolarization and increases spontaneous spiking of the OFF population [35, 36]. At 5 Hz, CdCl<sub>2</sub> again eradicated all activity, suggesting that RGCs are not directly activated by 5 Hz stimulation, but instead responses arise as the result of activation of presynaptic neurons. Similar to the response in ON cells, responses to 10 Hz stimulation persisted in OFF RGCs in the presence of CdCl<sub>2</sub>, supporting the notion that 10 Hz directly activates RGCs. However, the response patterns in the presence of CdCl<sub>2</sub> became sparser compared to under control conditions, suggesting that presynaptic neurons contribute to the observed control response. At 25 Hz, a similar amount of activity was observed under both control and in the presence of CdCl<sub>2</sub>, although a small phase shift was observed along with a change in the average inter-spike interval (analyzed below). Finally, the 100 Hz response was unchanged in the presence of CdCl<sub>2</sub> indicating



direct RGC activation. Responses of other cells in which blocker experiments were run (ON-BT  $n = 4$ , OFF-BT  $n = 4$ ) were similar to the examples shown.

When the results of the blocker experiments are taken together, they suggest that under control conditions the responses of RGCs to 5 and 10 Hz sinusoidal stimulation are the result of photoreceptor activation, the response to 25 Hz is primarily the result of RGC activation with a small contribution from presynaptic activation, and the response to 100 Hz is entirely the result of direct RGC activation. Interestingly, in the absence of photoreceptor activation (i.e. AP-4), only 5 Hz sinusoidal stimulation activated bipolar cells without also directly activating RGCs. This suggests that bipolar cells may be more difficult to selectively target than previously thought[22].

Examination of the OFF-BT and ON-BT responses in the presence of  $\text{CdCl}_2$  revealed that the inter-spike intervals (ISIs) of the responses appeared different at stimulus frequencies of 10 and 25 Hz. To quantify these differences, we plotted histograms of the ISI values (bin size of 0.1 ms) for responses of all cells in which the  $\text{CdCl}_2$  experiments were run (not shown). We then determined the bin in which the peak ISI occurred; the mean values are plotted in Fig. 7 for control (A) and in the presence of  $\text{CdCl}_2$  (B), where error bars represent standard deviation. Under control conditions, both cell types had peak ISIs at  $\sim 2$  ms for both 10 and 25 Hz. In the presence of  $\text{CdCl}_2$ , ON-BT cells maintained similar ISI values but the ISIs of OFF-BT responses increased, to  $5.54 \pm 1.34$  at 10 Hz at  $3.54 \pm 0.89$  at 25 Hz ( $p = 0.003$  for ON vs. OFF-BT at 10 Hz, and  $p = 0.025$  ON vs. OFF-BT at 25 Hz, one-way ANOVA). Because  $\text{CdCl}_2$  blocks all synaptic input (both excitatory and inhibitory), the ISI differences between ON and OFF BT cells suggest a difference in the intrinsic properties and/or firing mechanisms for the two cells. One possibility is the presence of an ion channel population that is sensitive to low frequency stimulation in ON-BT cells but not in OFF-BT cells.

## IV. DISCUSSION

While the results from this study continue to support the notion that sinusoidal waveforms may be a useful stimulus modality for retinal research, several new insights about the response of retinal neurons to such stimuli raise concerns about the clinical viability of such an approach. There were four primary findings that could be derived from the results of this study: 1) Different frequencies of stimulation activate different classes of retinal neurons, 2) Low frequencies produce different activity patterns in different types of RGC, 3) Low frequency sinusoids are more charge efficient than high frequency, and 4) The intrinsic spike generating mechanism within ON vs. OFF-BT cells is different. Each of these findings is discussed below. In addition, the potential limitations associated with the use of sinusoidal stimulation in a retinal prosthesis are discussed.

### A. Cellular targets of sinusoidal stimulation

The results of our experiments with pharmacological blockers suggest that under control conditions, 5 and 10 Hz sinusoidal stimulation activate photoreceptors, while 25 and 100 Hz directly activate RGCs. This differs from the findings of Freeman et al., who concluded that 5 Hz activates photoreceptors, 10 and 25 Hz activates bipolar cells, and 100 Hz activates

ganglion cells. Our conclusions were derived from utilization of the synaptic blockers AP-4 and CdCl<sub>2</sub>, as well as from visualization of changes in spike phases through the comparison of period overlay plots (Fig. 6); we believe this new approach enabled a more complete and accurate determination of cellular targets than the previous study. Notably, because the frequencies examined here did not activate bipolar cells without also activating either photoreceptors or ganglion cells, our results suggest that bipolar cells may be more difficult to selectively target than previously thought, and are likely to have relatively high activation thresholds under control conditions. These findings are consistent with previous work[37] that suggested that photoreceptors were the neurons activated by indirect activation in the healthy retina, although other work has characterized the ability to selectively activate different cell populations using different stimuli and electrode placements for pulsatile stimuli [23]. However, our results also suggest that when photoreceptors are blocked via AP-4, 5 Hz stimulation is capable of activating bipolar cells without also activating RGCs. Presumably, this will also be the case when photoreceptors are degraded in the degenerate retina, however due to significant rewiring of retinal connections during degeneration [38, 39], this will need to be verified experimentally.

In the case of 25 Hz, the target of activation was less clear than that of other frequencies. For example, in the 25 Hz responses seen in Fig. 6A, the cell produced 7 spikes per period in control conditions, 6 in the presence of AP-4, and 5 when CdCl<sub>2</sub> was added to the bath. Analysis of all other cells tested (n = 4) showed qualitatively consistent results: similarly small but statistically significant decreases in activity occurred when each synaptic blocker was successively applied. Therefore, while the control response appears to be primarily mediated by direct RGC activation, there does seem to be an additional component of the response that arises from presynaptic input. The small reduction in activity that occurred when CdCl<sub>2</sub> was added to the AP-4 may be attributable to blockage of some sort of tonic excitatory input to RGCs, likely mediated through bipolar cells. This input would depolarize the RGC thereby increasing its excitability and resulting in more spikes. It is more difficult however to explain the small reduction in spiking that occurred when AP-4 was originally added to the bath. Because the elicited activity occurred during the cathodal phase in an ON cell, the photoreceptors should be depolarized – this should result in hyperpolarization of the bipolar cells and a resultant *decrease* in the excitability of the RGC. We were not able to reconcile this discrepancy, although the possibility exists that other neural populations along the synaptic pathway contribute to the increase in excitability observed under control conditions.

The ability of each frequency of sinusoidal stimulation to activate axons was not examined in this study. However, when combined with the results of Freeman et al[22] regarding axonal activation, our results suggest that 25 Hz sinusoids are able to directly activate RGCs while simultaneously avoiding axonal activation. This could potentially allow for fast video coding while still creating spatially precise percepts.

The occurrence of multiple spikes per phase in the presence of cadmium during 10 and 25 Hz stimulation was somewhat surprising, as multiple spikes per stimulus are commonly associated with network activation, while direct activation is typically associated with one spike[24, 40-43]. While there is the possibility of an incomplete block via cadmium, this

seems unlikely given much previous verification of its effectiveness[34, 43, 44]. Instead, it seems more likely that the relatively short durations of pulses used for direct activation studies accounts for the lack of observation of multiple spikes; when longer duration stimuli are used, such as low-frequency sinusoids, it becomes possible to elicit multiple spikes through direct activation. Further support for this notion can be seen in Fig. 3 (OFF-BT cell, top right panel) where the 100 Hz stimulus (direct activation only) produced two spikes per phase. These findings are consistent with previous evidence suggesting that multiple spikes can arise even without network activation[42].

Our results also suggest that activation of one type of neuron within the retinal circuitry may inhibit the responses arising from simultaneous activation of other downstream neurons. For example, when the synaptic blocker experiments were run for ON-BT cells at 5 Hz (Fig. 6A, first column), there was no spiking response in the RGC in the presence of CdCl<sub>2</sub>, suggesting activity was not created directly in the RGC. Thus the spiking that occurred when input from photoreceptors was blocked by AP-4 was almost certainly the result of bipolar cell activation. This activity (in AP-4) occurred during the cathodal phase and was therefore in contrast to the anodal phase activity arising from photoreceptor activation under control conditions. This raises the question of why only the photoreceptor-mediated component is present in the control response if the activation of bipolar cells occurs during the other phase of the 5 Hz stimulus. A likely explanation for this is the sign-inverting synapse: during the cathodal phase of the sinusoid, the photoreceptors are depolarized, which hyperpolarizes the bipolar cells and prevents them from being activated. This would suggest therefore that the inhibitory input arriving at bipolar cells in response to photoreceptor depolarization is strong enough to override the direct excitatory effect arising from the stimulus onto the bipolar cell itself. It will be interesting to further explore other interactions that occur when multiple classes of retinal neurons are simultaneously activated. It will be especially important to understand the interactions that arise in RGCs in response to simultaneous activation of excitatory bipolar cells and inhibitory amacrine cells, and whether there are ways to shift the balance more toward one cell population or another.

## B. Responses differ for different types of RGCs

We observed differences in the phase at which spiking occurred between ON and OFF cells, particularly at low frequencies (Fig. 5). For sustained cells, there was a small phase difference between ON and OFF cells, while for BT cells, the ON vs. OFF phase differences were larger:  $\sim 160^\circ$  at 5Hz,  $\sim 145^\circ$  at 10 Hz,  $\sim 90^\circ$  at 25 Hz, and  $\sim 0^\circ$  at 100 Hz. These phase differences were qualitatively larger than those found by Freeman et al. (e.g. compare Figure 6 of the present study to Fig. 6e of Freeman). Although Freeman et al. determined the phase of peak activity while our study analyzed the first spike phase, this difference in methods would alter the results by only several degrees, and therefore does not account for the discrepancy between the two sets of findings. Instead, the fact that BT and sustained cells were averaged together in the Freeman study likely explains the smaller phase differences than those found here. Importantly, because the response of RGCs to 25 Hz is primarily the result of direct ganglion cell activation (Fig. 6A), the  $\sim 90^\circ$  phase difference observed between ON and OFF-BT cells likely represents an as yet undetermined difference in the ON vs. OFF pathway, i.e. it does not arise from the sign-inverting synapse between the ON

photoreceptors and bipolar cells. As photoreceptors are not generally a viable target for stimulation in the degenerate retina, any response difference that does not involve photoreceptors is of greater potential utility for creating physiological-like activity with a clinical device. Because the 25 Hz phase difference disappeared in the presence of CdCl<sub>2</sub> (Fig. 6B, 25 Hz), however, it likely does not reflect a difference in the inherent ion channel properties of ON vs. OFF-BT cells. Instead, it is likely to reflect a difference in the sensitivity in either the bipolar cells that supply each type and/or a difference in the synaptic circuitry supplying ON vs. OFF BT cells.

Responses of ON-SUST cells were unique among the 4 cell types examined in that they responded poorly to low frequency sinusoidal stimulation (Fig. 3). There are two reasons why this finding may be significant. First, the ability to selectively target one type of sustained cell at low frequencies (OFF but not ON) may be highly useful in portions of the retina where such cells are known to be the dominant population, i.e. the primate fovea. Second, because similar levels of activity were created in OFF-BT, OFF-SUST, and ON-BT cells, but not in ON-SUST cells, this suggests that ON-SUST cells have a unique circuit or mode of activation relative to the other cell types. Our results do not directly address the reason(s) for the response weakness, but one possible explanation is the existence of an inhibitory mechanism unique to the ON-SUST pathway that is sensitive to low frequency stimulation. Previous studies have shown inhibitory mechanisms that are specific to distinct RGC populations [45-47], raising the possibility that an as yet unidentified inhibitory signal similarly exists in the ON-SUST circuitry. The fact that ON-SUST cells had significantly different response characteristics from ON-BT cells strongly supports the need to further classify RGC types, beyond basic ON vs. OFF characterization, in studies that explore retinal responses to prosthetic stimulation.

### C. Photoreceptor activation is more charge efficient than direct RGC activation

By comparing the number of spikes elicited at each stimulus frequency, we were able to calculate the mean charge per spike as a function of frequency (Fig. 4E, dotted line, right axis). These results suggest that the activation of photoreceptors via low frequency sinusoidal stimulation creates more action potentials in RGCs per unit charge than does direct activation of the RGC via higher frequencies; therefore low frequency stimulations are more charge efficient than high frequency. This was surprising, as these recordings were taken in the epiretinal configuration in which the stimulating electrode was closer to the RGC layer, and thus further from the photoreceptor layer. Had these experiments been performed in the subretinal configuration, it is possible that low frequencies would have proven even more charge efficient. Recent work from Lee et. al. has shown that for pulsatile stimulation, short pulses produce more activity than long pulses of the same charge when applied subretinally [48]. However the Lee study took into account spikes that occurred after the termination of the stimulus, suggesting that results between the two studies cannot be directly compared.

### D. ISI Differences in ON vs. OFF BT cells

The results of the synaptic blocker experiments revealed that in the presence of CdCl<sub>2</sub>, ON and OFF-BT responses to 10 and 25 Hz sinusoidal stimulation produced activity with

differing peak ISIs values (Fig. 7B). Specifically, at 10 Hz, OFF cells exhibited ISIs that were 152% longer than those of ON cells; at 25 Hz, OFF ISIs were 67% longer than ON ISIs. Because all synaptic input (both excitatory and inhibitory) was blocked by CdCl<sub>2</sub>, these results hint at an intrinsic difference within the two types of ganglion cells, and may result from the presence of one or more types of low frequency sensitive ion channels in ON-BT cells that are absent in OFF-BT cells. To date, the only definitive difference that has been identified in the intrinsic ion channel properties of ON and OFF cells is the presence of a low-voltage activated (LVA) Ca<sup>2+</sup> ion channels in OFF ganglion cells and are absent in ON cells [49]. However this channel does not seem a likely candidate to explain our results, since ON cells were able to fire faster than OFF cells in our experiments. Determination of the precise mechanism behind this phenomenon is left for future studies.

### E. Potential Drawbacks

Our study revealed several features of low frequency sinusoidal stimulation that may hinder the usefulness of such a stimulation strategy in a retinal prosthesis. First, our results indicate that the primary site of activation for low frequency sinusoids is the photoreceptors, a target that is not viable in the degenerate retina where retinal prostheses are utilized. However, our results suggest that in the absence of photoreceptor activation, low frequency sinusoids will instead activate bipolar cells, making it possible that such waveforms might be useful, although further testing will be necessary to determine if this type of indirect stimulation will persist in the degenerate retina. In addition, it is important to keep in mind that retinal rewiring due to degeneration [38, 39] may further complicate the response, e.g. for those frequencies that activate the network. Second, it is questionable as to whether the lowest frequencies tested here are truly a viable stimulation strategy, since frame-rates of >20Hz are generally required for effective video encoding. Interestingly however, patients claim to prefer refresh rates of 5-7 Hz during clinical trials with retinal prosthetics [2, 9] suggesting that low rates should not be immediately discounted. Finally, the inability to effectively activate ON-SUST cells may represent another significant drawback of low frequency sinusoids. ON-SUST cells in rabbit are the homologs of ON midget cells in primate, raising the possibility that this important cell type for human vision is not effectively activated by low frequency sinusoids. It will be interesting in future studies with the degenerate retina to examine the retinal responses to low frequency sinusoidal stimulation in order to determine whether some or all of these limitations can be overcome.

### ACKNOWLEDGEMENTS

We would like to thank Maesoon Im, Seung Woo Lee, and Eva Shirley Sanchez for helpful discussion.

This research was supported by the VA Boston Healthcare system (1I01RX000350-01A1) as well as the NIH (1R01 EY019967-01).

### References

1. Ahuja AK. Blind subjects implanted with the Argus II retinal prosthesis are able to improve performance in a spatial-motor task. *Br. J. Ophthalmol.* 2011; 95:539–543. [PubMed: 20881025]
2. Zrenner E, Bartz-Schmidt KU, Benav H, Besch D, Bruckmann A, Gabel VP, et al. Subretinal electronic chips allow blind patients to read letters and combine them to words. *Proc Biol Sci.* May 22.2011 278:1489–97. [PubMed: 21047851]

3. Habib AG, Cameron MA, Suaning GJ, Lovell NH, Morley JW. Spatially restricted electrical activation of retinal ganglion cells in the rabbit retina by hexapolar electrode return configuration. *J Neural Eng.* Jun.2013 10:036013. [PubMed: 23612906]
4. Mathieson K, Loudin J, Goetz G, Huie P, Wang L, Kamins TI, et al. Photovoltaic Retinal Prosthesis with High Pixel Density. *Nat Photonics.* Jun 1.2012 6:391–397. [PubMed: 23049619]
5. Tokuda T, Ito T, Kitao T, Noda T, Sasagawa K, Terasawa Y, et al. CMOS-based smart-electrode-type retinal stimulator with bullet-shaped bulk Pt electrodes. *Conf Proc IEEE Eng Med Biol Soc.* 20112011:6733–6. [PubMed: 22255884]
6. Villalobos J, Nayagam DA, Allen PJ, McKelvie P, Luu CD, Ayton LN, et al. A wide-field suprachoroidal retinal prosthesis is stable and well tolerated following chronic implantation. *Invest Ophthalmol Vis Sci.* May.2013 54:3751–62. [PubMed: 23611996]
7. Lee SW, Seo JM, Ha S, Kim ET, Chung H, Kim SJ. Development of microelectrode arrays for artificial retinal implants using liquid crystal polymers. *Invest Ophthalmol Vis Sci.* Dec.2009 50:5859–66. [PubMed: 19553608]
8. daCruz L, Coley B, Christopher P, Merlini F, Wuyyuru V, Sahel JA, et al. Patients Blinded by Outer Retinal Dystrophies Are Able to Identify Letters Using the Argus II Retinal Prosthesis System. *Invest. Ophthalmol. Vis. Sci.* 51 Abstract #: 2023, 2010.
9. Stingl K, Bartz-Schmidt KU, Besch D, Braun A, Bruckmann A, Gekeler F, et al. Artificial vision with wirelessly powered subretinal electronic implant alpha-IMS. *Proc Biol Sci.* 2013; 280:20130077. [PubMed: 23427175]
10. Wilson BS, Dorman MF. Cochlear implants: current designs and future possibilities. *J Rehabil. Res. Dev.* 2008; 45:695–730. [PubMed: 18816422]
11. Perlmutter JS, Mink JW. Deep brain stimulation. *Annu Rev Neurosci.* 2006; 29:229–57. [PubMed: 16776585]
12. Beck H, Boden WE, Patibandla S, Kireyev D, Gutpa V, Campagna F, et al. 50th Anniversary of the first successful permanent pacemaker implantation in the United States: historical review and future directions. *Am J Cardiol.* Sep 15.2010 106:810–8. [PubMed: 21391322]
13. Weiland JD, Liu W, Humayun MS. Retinal prosthesis. *Annu Rev Biomed Eng.* 2005; 7:361–401. [PubMed: 16004575]
14. Behrend MR, Ahuja AK, Humayun MS, Weiland JD, Chow RH. Selective labeling of retinal ganglion cells with calcium indicators by retrograde loading in vitro. *J Neurosci Methods.* May 15.2009 179:166–72. [PubMed: 19428523]
15. Fried SI, Hsueh HA, Werblin FS. A method for generating precise temporal patterns of retinal spiking using prosthetic stimulation. *J Neurophysiol.* Feb.2006 95:970–8. [PubMed: 16236780]
16. Jensen RJ, Rizzo JF 3rd, Ziv OR, Grumet A, Wyatt J. Thresholds for activation of rabbit retinal ganglion cells with an ultrafine, extracellular microelectrode. *Invest Ophthalmol Vis Sci.* Aug.2003 44:3533–43. [PubMed: 12882804]
17. Jensen RJ, Ziv OR, Rizzo JF. Responses of rabbit retinal ganglion cells to electrical stimulation with an epiretinal electrode. *J Neural Eng.* Mar.2005 2:S16–21. [PubMed: 15876650]
18. Busskamp V, Duebel J, Balya D, Fradot M, Viney TJ, Siebert S, et al. Genetic reactivation of cone photoreceptors restores visual responses in retinitis pigmentosa. *Science.* Jul 23.2010 329:413–7. [PubMed: 20576849]
19. Fried SI, Lasker AC, Desai NJ, Eddington DK, Rizzo JF 3rd. Axonal sodium-channel bands shape the response to electric stimulation in retinal ganglion cells. *J Neurophysiol.* Apr.2009 101:1972–87. [PubMed: 19193771]
20. Sekirnjak C, Hottowy P, Sher A, Dabrowski W, Litke AM, Chichilnisky EJ. High-resolution electrical stimulation of primate retina for epiretinal implant design. *J Neurosci.* Apr 23.2008 28:4446–56. [PubMed: 18434523]
21. Freeman DK, Jeng JS, Kelly SK, Hartveit E, Fried SI. Calcium channel dynamics limit synaptic release in response to prosthetic stimulation with sinusoidal waveforms. *J Neural Eng.* May 31.2011 8:046005. [PubMed: 21628768]
22. Freeman DK, Eddington DK, Rizzo JF, Fried SI. Selective activation of neuronal targets with sinusoidal electric stimulation. *Journal of Neurophysiology.* 2010; 104:2778–2791. [PubMed: 20810683]



23. Boinagrov D, Pangratz-Fuehrer S, Goetz G, Palanker D. Selectivity of direct and network-mediated stimulation of the retinal ganglion cells with epi-, sub- and intraretinal electrodes. *J Neural Eng.* Apr.2014 11:026008. [PubMed: 24608166]
24. Freeman DK, Fried SI. Multiple components of ganglion cell desensitization in response to prosthetic stimulation. *J Neural Eng.* Feb.2011 8:016008. [PubMed: 21248379]
25. Jensen RJ, Rizzo JF 3rd. Responses of ganglion cells to repetitive electrical stimulation of the retina. *J Neural Eng.* Mar.2007 4:S1–6. [PubMed: 17325407]
26. Jensen RJ, Ziv OR, Rizzo JF 3rd, Scribner D, Johnson L. Spatiotemporal aspects of pulsed electrical stimuli on the responses of rabbit retinal ganglion cells. *Exp Eye Res.* Dec.2009 89:972–9. [PubMed: 19766116]
27. Roska B, Werblin F. Vertical interactions across ten parallel, stacked representations in the mammalian retina. *Nature.* Mar 29.2001 410:583–587. [PubMed: 11279496]
28. Cleland BG, Levick WR. Brisk and sluggish concentrically organized ganglion cells in the cat's retina. *J Physiol.* Jul.1974 240:421–56. [PubMed: 4421622]
29. DeVries SH, Baylor DA. Mosaic arrangement of ganglion cell receptive fields in rabbit retina. *Journal of Neurophysiology.* Oct.1997 78:2048–2060. [PubMed: 9325372]
30. Brummer SB, Turner MJ. Electrical stimulation with Pt electrodes: II-estimation of maximum surface redox (theoretical non-gassing) limits. *IEEE Trans Biomed Eng.* Sep.1977 24:440–3. [PubMed: 892838]
31. Schiller PH. Central connections of the retinal ON and OFF pathways. *Nature.* Jun 17.1982 297:580–3. [PubMed: 7088141]
32. Shiells RA, Falk G, Naghshineh S. Action of glutamate and aspartate analogues on rod horizontal and bipolar cells. *Nature.* Dec 10.1981 294:592–4. [PubMed: 6273752]
33. Slaughter MM, Miller RF. 2-amino-4-phosphonobutyric acid: a new pharmacological tool for retina research. *Science.* Jan 9.1981 211:182–5. [PubMed: 6255566]
34. Margalit E, Thoreson WB. Inner retinal mechanisms engaged by retinal electrical stimulation. *Invest Ophthalmol Vis Sci.* Jun.2006 47:2606–12. [PubMed: 16723477]
35. Margolis DJ, Detwiler PB. Different mechanisms generate maintained activity in ON and OFF retinal ganglion cells. *J Neurosci.* May 30.2007 27:5994–6005. [PubMed: 17537971]
36. Zaghoul KA, Boahen K, Demb JB. Different circuits for ON and OFF retinal ganglion cells cause different contrast sensitivities. *J Neurosci.* Apr 1.2003 23:2645–54. [PubMed: 12684450]
37. Margalit E, Babai N, Luo J, Thoreson WB. Inner and outer retinal mechanisms engaged by epiretinal stimulation in normal and rd mice. *Visual neuroscience.* 2011; 28:145–154. [PubMed: 21463541]
38. Marc RE, Jones BW, Watt CB, Strettoi E. Neural remodeling in retinal degeneration. *Prog Retin Eye Res.* Sep.2003 22:607–55. [PubMed: 12892644]
39. Jones BW, Marc RE. Retinal remodeling during retinal degeneration. *Exp Eye Res.* Aug.2005 81:123–37. [PubMed: 15916760]
40. Jensen RJ, Ziv OR, Rizzo JF. Thresholds for activation of rabbit retinal ganglion cells with relatively large, extracellular microelectrodes. *Investigative ophthalmology & visual science.* 2005; 46:1486–1496. [PubMed: 15790920]
41. Fried SI, Hsueh H-A, Werblin FS. A method for generating precise temporal patterns of retinal spiking using prosthetic stimulation. *Journal of neurophysiology.* 2006; 95:970–978. [PubMed: 16236780]
42. Sekirnjak C, Hottowy P, Sher A, Dabrowski W, Litke A, Chichilnisky E. Electrical stimulation of mammalian retinal ganglion cells with multielectrode arrays. *Journal of neurophysiology.* 2006; 95:3311–3327. [PubMed: 16436479]
43. Tsai D, Morley JW, Suaning GJ, Lovell NH. Direct activation and temporal response properties of rabbit retinal ganglion cells following subretinal stimulation. *Journal of neurophysiology.* 2009; 102:2982–2993. [PubMed: 19741103]
44. Cohen ED. Voltage-gated calcium and sodium currents of starburst amacrine cells in the rabbit retina. *Visual neuroscience.* 2001; 18:799–809. [PubMed: 11925015]

45. Pang JJ, Gao F, Wu SM. Light-evoked excitatory and inhibitory synaptic inputs to ON and OFF alpha ganglion cells in the mouse retina. *J Neurosci.* Jul 9.2003 23:6063–73. [PubMed: 12853425]
46. Manookin MB, Beaudoin DL, Ernst ZR, Flagel LJ, Demb JB. Disinhibition combines with excitation to extend the operating range of the OFF visual pathway in daylight. *J Neurosci.* Apr 16.2008 28:4136–50. [PubMed: 18417693]
47. Newkirk GS, Hoon M, Wong RO, Detwiler PB. Inhibitory inputs tune the light response properties of dopaminergic amacrine cells in mouse retina. *Neurophysiol.* Jul.2013 110:536–52.
48. Lee SW, Eddington DK, Fried SI. Responses to pulsatile subretinal electric stimulation: effects of amplitude and duration. *J Neurophysiol.* Apr.2013 109:1954–68. [PubMed: 23343891]
49. Margolis DJ, Gartland AJ, Euler T, Detwiler PB. Dendritic calcium signaling in ON and OFF mouse retinal ganglion cells. *J Neurosci.* May 26.2010 30:7127–38. [PubMed: 20505081]
50. Goldberg EM, Clark BD, Zaghera E, Nahmani M, Erisir A, Rudy B. K+ channels at the axon initial segment dampen near-threshold excitability of neocortical fast-spiking GABAergic interneurons. *Neuron.* May 8.2008 58:387–400. [PubMed: 18466749]

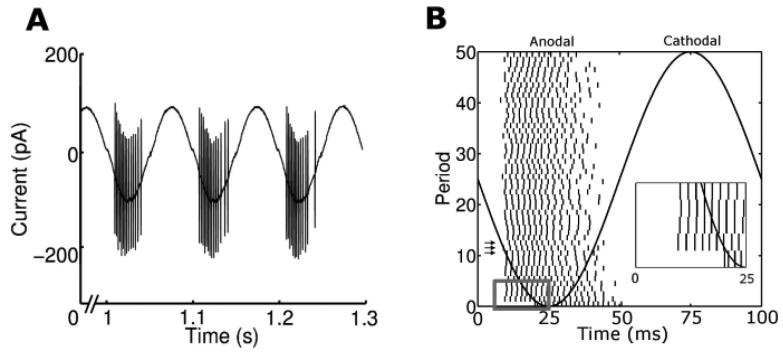


**Fig. 1.** Period overlays allow the consistency of spike timing to be visualized across periods. (A) Raw recording of a portion of the response from an ON-BT cell to 10 Hz sinusoidal stimulation; action potentials embedded within the sinusoidal artifact are clearly visible. (B) Spike times are extracted from the raw signal and are plotted such that the spikes elicited by a single period of the waveform are plotted on a single row; successive periods are displayed from bottom to top. The sinusoidal waveform is overlaid, anodal phase first, so that spike timing can be correlated with the sinusoidal phase during which it occurs. Inset shows an expanded view of the first 5 periods (grey box). Arrows denote the three periods shown in panel (A)

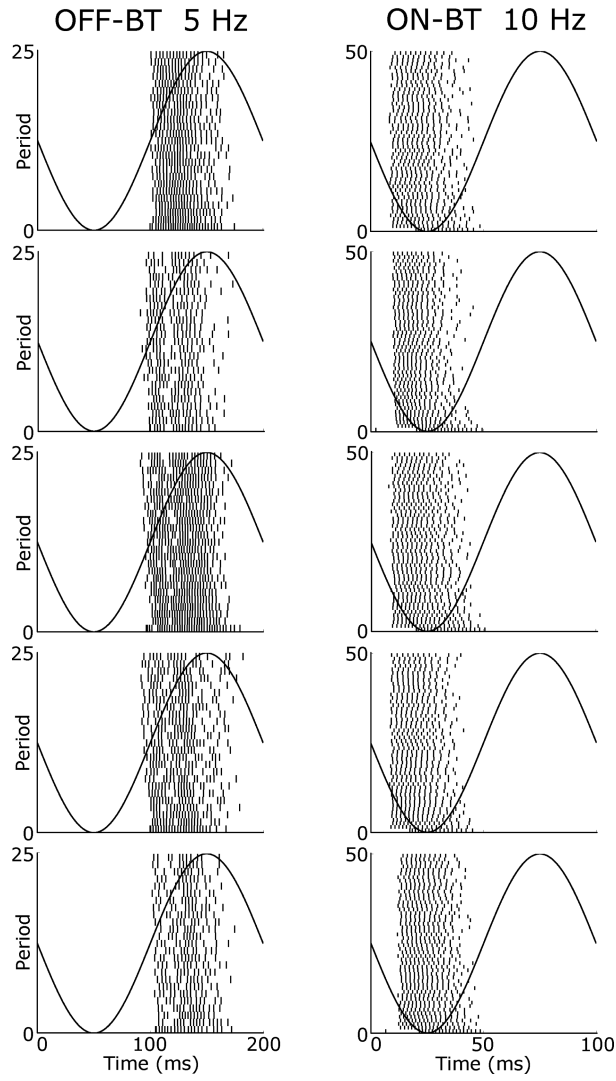


**Fig. 2.** Sinusoidal responses are highly similar across RGCs of a given type. Period overlays are shown for 5 different OFF-BT cells in response to 5 Hz stimulation (left column) and 5 different ON-BT cells in response to 10 Hz stimulation (right column).

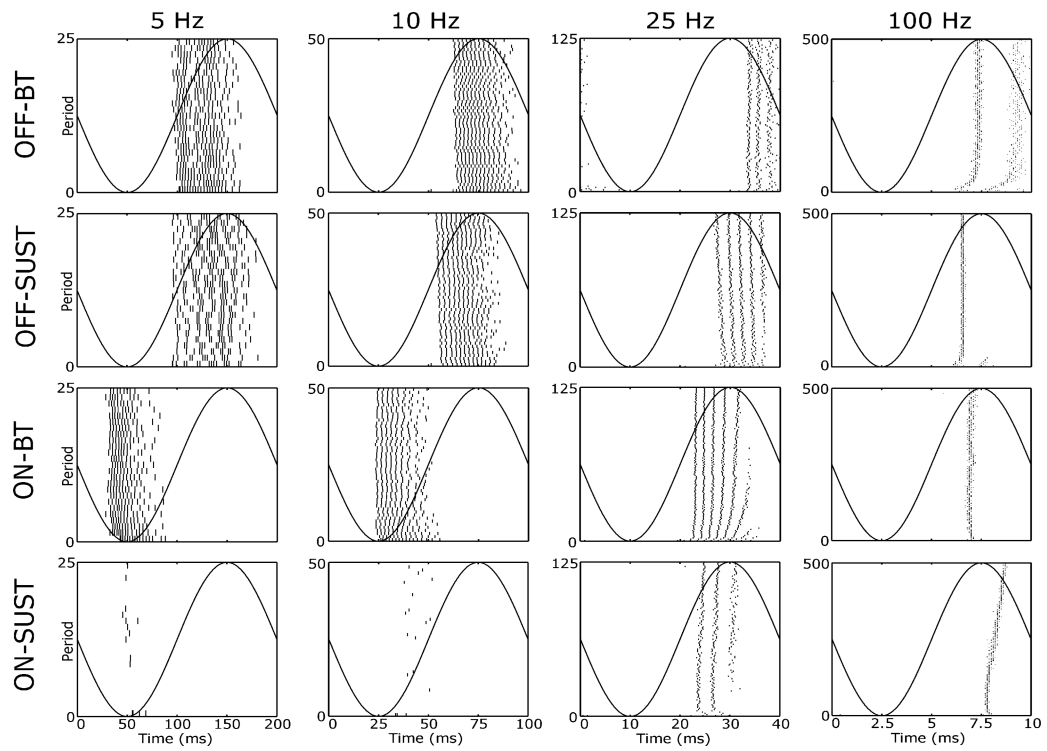


**Fig. 3.** Sinusoidal stimulation produces different activity patterns in different types of RGCs. Representative period overlays of OFF-BT (top row), OFF-SUST (2<sup>nd</sup> row), ON-BT (3<sup>rd</sup> row), and ON-SUST (bottom row) responses to 5, 10, 25, and 100 Hz sinusoidal stimulation.

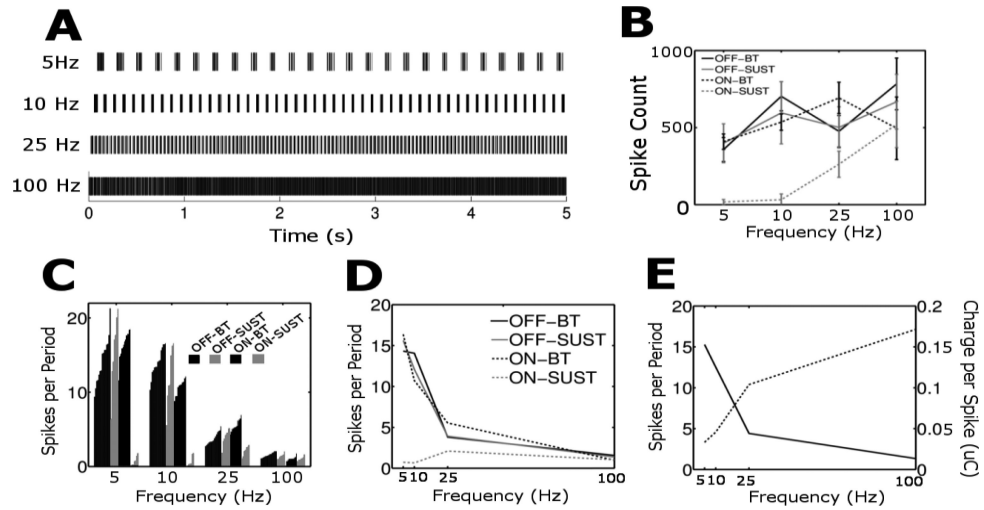


**Fig. 4.** Low frequency sinusoidal stimuli are more charge efficient than high frequency. (A) Spike raster plots of a single OFF-BT cell in response to 5-second sinusoidal stimulation at the four frequencies indicated. (B) Average total spike count per 5-second stimulus as a function of stimulus frequency. Error bars represent  $\pm$  SD (C) Each vertical bar represents the average spikes per period for one cell. For each frequency, cells are arranged in ascending order of spike count and separated by cell type. (D) Mean spikes per period averaged over each cell type and plotted as a function of frequency. (E) Mean spikes per period averaged across all OFF-BT, OFF-SUST, and ON-BT cells (solid line, left axis), and mean charge per spike for the same cell populations (dotted line, right axis).



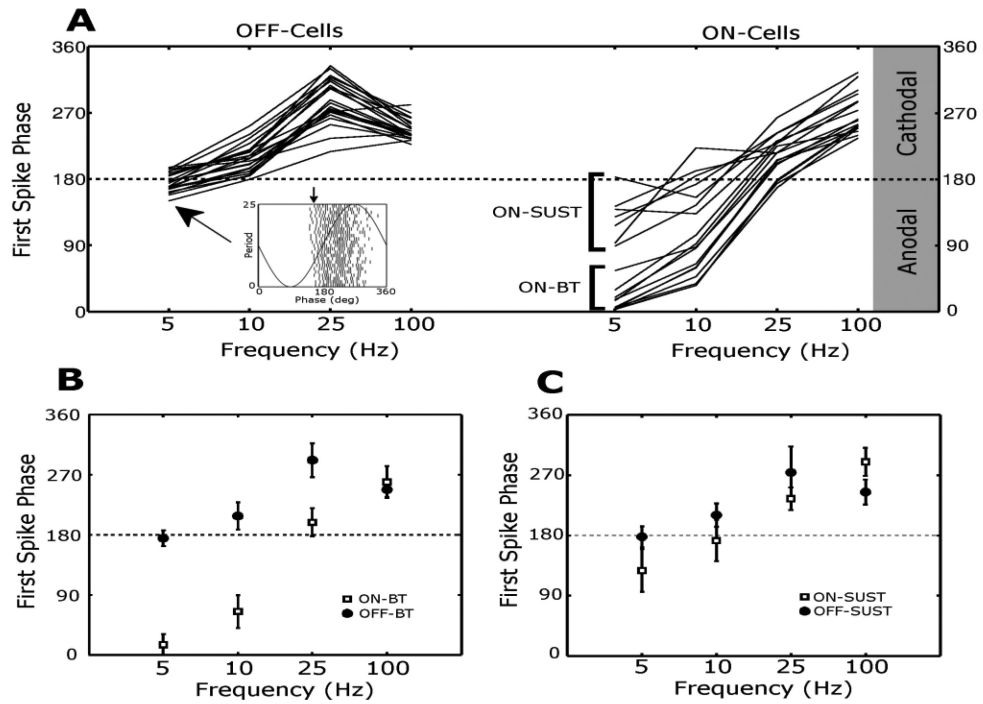


**Fig. 5.** Sinusoidal stimulation elicits activity at different phases in different RGC types. (A) Each point plots the average phase of the sinusoidal waveform at which the first spike occurred. Each line connects the data points of a single cell as a function of frequency; ON and OFF cells are plotted separately, as indicated. Inset shows a period overlay of an OFF-SUST response to 5 Hz stimulation where the mean first spike phase is marked with the small arrow. This phase value corresponds to the data point indicated by the large arrow. (B) Mean first spike phases are shown averaged over all BT-type cells, and (C) all SUST-type cells. Error bars represent  $\pm$ SD.

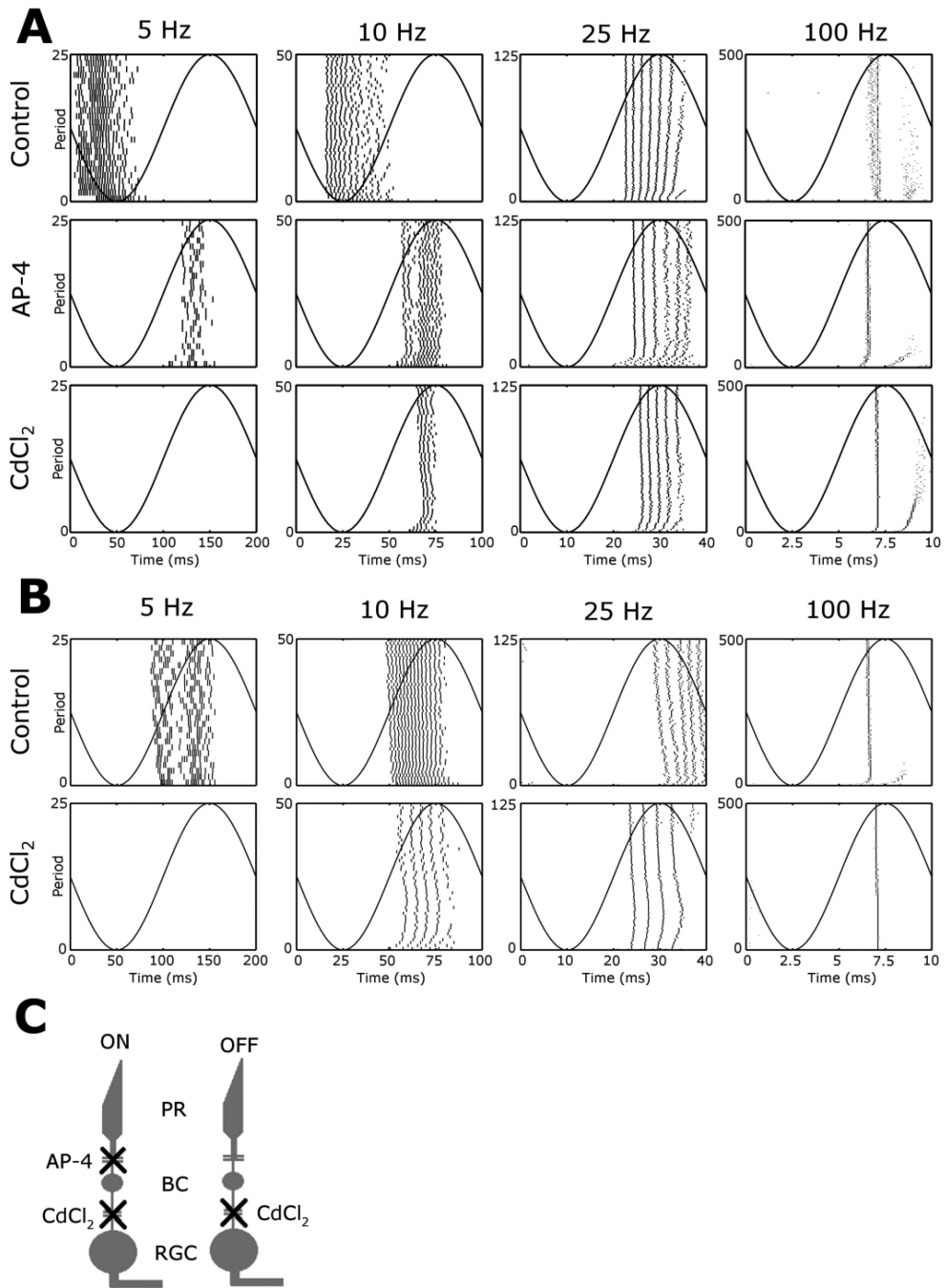


**Fig. 6.** Synaptic blockers reveal cellular origins of activity. Period overlays for a single ON-BT cell (A) and OFF-BT cell (B) at the stimulus frequencies indicated at top; measurements were made under control conditions and in the presence of synaptic blockers AP-4 or CdCl<sub>2</sub> as indicated at left. (C) Cartoon illustrating the effects of synaptic blockers in the ON (left) and OFF (right) pathways where photoreceptors (PR), bipolar cells (BC), and retinal ganglion cells (RGC) are labeled.

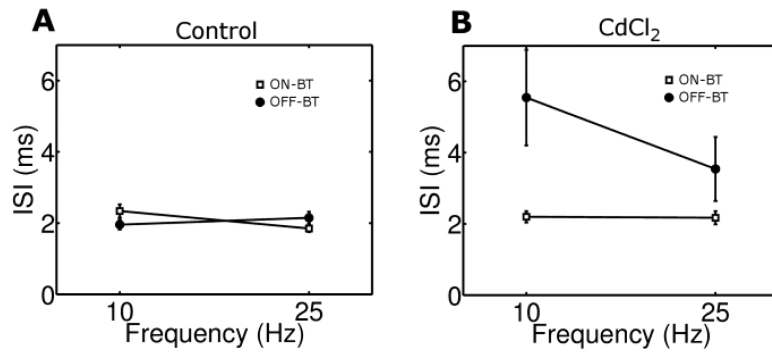


**Fig. 7.** Inter-spike interval [50] values differ between ON and OFF-BT cells when synaptic input is blocked. Mean peak ISI for ON and OFF-BT cells during sinusoidal stimulation at 10 and 25 Hz in control conditions (A) and in the presence of CdCl<sub>2</sub> (B). Error bars represent  $\pm$  SD

Author Manuscript

Author Manuscript

Author Manuscript

Author Manuscript